

# On the role of different Skyrme forces and surface corrections in exotic cluster-decay

Narinder K. Dhiman\*  
 Govt. Sr. Sec. School,  
 Summer Hill, Shimla -171005, (India)

Ishwar Dutt  
 Department of Physics, Panjab University,  
 Chandigarh -160014, (India)

(Dated: August 28, 2018)

We present cluster decay studies of  $^{56}\text{Ni}^*$  formed in heavy-ion collisions using different Skyrme forces. Our study reveals that different Skyrme forces do not alter the transfer structure of fractional yields significantly. The cluster decay half-lives of different clusters lies within  $\pm 10\%$  for PCM and  $\pm 15\%$  for UFM.

PACS numbers: 25.70Jj, 23.70+j, 24.10-i, 23.60+e.

## I. INTRODUCTION

Recently, a renewed interest has emerged in nuclear physics research. This includes low energy fusion process [1], intermediate energy phenomena [2] as well as cluster-decay and/or formation of super heavy nuclei [3, 4]. In the last one decade, several theoretical models have been employed in the literature to estimate the half-life times of various exotic cluster decays of radioactive nuclei. These outcome have also been compared with experimental data. Most of these models applied to study exotic cluster decay can be classified into two categories: In the first category, only barrier penetration probabilities are considered. Such models have been labeled as unified fission models (UFM) [5–7]. In the second category, clusters are assumed to be formed well before penetration. This is done by including the preformation probability in the calculations. These models have been dubbed as preformed cluster models (PCM) [8–10]. In either of these approach, one needs complete knowledge of the potential.

This problem is tackled in the literature in two different manners: One tries to adjust various parameters of model to known experimental data [11–14]. Alternatively, one starts from a basic fundamental approach free from such adjustable parameters [15–21]. It remain to be seen how particular set of model parameters influence the cluster decay process. We plan to address this question in this paper. We shall work out the above problem with potential obtained from the Skyrme interactions. The Skyrme interactions are well used to describe the fusion process at low incident energies as well as in subthreshold, collective flow, and multifragmentation at intermediate energies.

The Skyrme force is an effective interaction, which parameterizes the  $G$ -matrix by a zero range, density and momentum dependent ansatz. The Skyrme force consists of two-body as well as three-body parts as [20]:

$$V = \sum_{i<j} v_{ij} + \sum_{i<j<k} v_{ijk}. \quad (1)$$

Using a short-range expansion of the two-body interaction, the matrix elements in momentum space can be written as:

$$\langle \vec{k} | v_{12} | \vec{k}' \rangle = t_0 (1 + x_0 P_\sigma) + \frac{1}{2} t_1 (k^2 + k'^2) + t_2 \vec{k} \cdot \vec{k}' + iW_0 (\vec{\sigma}_1 + \vec{\sigma}_2) \cdot \vec{k} \times \vec{k}', \quad (2)$$

where  $\vec{k}$  and  $\vec{k}'$  are the relative wave vectors of the nucleons.  $P_\sigma$  is spin exchange operator and  $\vec{\sigma}$  are Pauli spin matrices. To deal with such interaction, it is convenient to write the matrix elements in configuration space as:

$$v_{12} = t_0 (1 + x_0 P_\sigma) \delta(\vec{r}_1 - \vec{r}_2) + \frac{1}{2} t_1 [\delta(\vec{r}_1 - \vec{r}_2) k^2 + k'^2 \delta(\vec{r}_1 - \vec{r}_2)] \\ + t_2 \vec{k}' \cdot \delta(\vec{r}_1 - \vec{r}_2) \vec{k} + iW_0 (\vec{\sigma}_1 + \vec{\sigma}_2) \cdot \vec{k}' \times \delta(\vec{r}_1 - \vec{r}_2) \vec{k}, \quad (3)$$

---

\*Electronic address: narinder.dhiman@gmail.com

here  $\vec{k}(= (\vec{\nabla}_1 - \vec{\nabla}_2)/2\iota)$  denotes the relative momentum operators acting on the right and  $\vec{k}'(= -(\vec{\nabla}_1 - \vec{\nabla}_2)/2\iota)$ , acting on left, respectively.

The three-body term of the Skyrme force can be written as:

$$v_{123} = t_3 \delta(\vec{r}_1 - \vec{r}_2) \delta(\vec{r}_2 - \vec{r}_3). \quad (4)$$

For the Hartree-Fock calculations of even-even nuclei, this force is shown to be equivalent to a two-body density dependent interaction:

$$v_{12} = \frac{1}{6} t_3 (1 + P_\sigma) \delta(\vec{r}_1 - \vec{r}_2) \rho \left( \frac{\vec{r}_1 + \vec{r}_2}{2} \right). \quad (5)$$

The above form, Eq. (5), provides a simple phenomenological representation of many body effects describing the way, in which the interaction between two nucleons is influenced by the presence of others. The Skyrme interaction is an approximate representation of the effective nucleon force which is valid only for the low relative momentum. In Eqs. (2) to (5), we see several constants/parameters like  $t_0$ ,  $t_1$ ,  $t_2$ ,  $t_3$ ,  $x_0$ , and  $W_0$  that need to be fitted. These parameters have been fitted by various authors from time to time to get better description of various ground state properties of nuclei [17, 20–22]. A particular set comprising these parameters is known as *Skyrme force*. Till to-date, large number of Skyrme forces are available in the literature [22]. These different Skyrme forces constituting different equation of state at intermediate energies[23, 24]. All the conventional (i.e. with the three body term replaced by a density dependent two body term), generalized (adjusting the effective mass  $m^*$  and compressibility  $K$ ) and modified Skyrme forces (adjusting the density parameter  $t_3$  to fit the spectra) are unified in a single form by Zhuo [25] as an extended Skyrme force.

$$V_{ES} = \sum_{i < j} v_{ij}. \quad (6)$$

Our aim here is to study the role of various Skyrme forces and surface corrections in the exotic cluster decay process. This study is still missing in the literature.

In recent years, there have been a number of experimental and theoretical studies [26–38] aimed at understanding the decay of light compound nucleus formed through heavy-ion reactions. In most of the reactions studied, whereas the general conclusion about the formation probability for the compound nucleus and characteristic features of its decay are debated in terms of either fusion-fission mechanism [26, 28, 39], which may be considered as the emission of complex (or intermediate mass) fragments, or a deep inelastic (DI) orbiting [40] mechanism behaviour.

One of such system is the doubly magic  $^{56}\text{Ni}$ , which is studied by using several entrance channels ( $^{16}\text{O} + ^{40}\text{Ca}$ ,  $^{32}\text{S} + ^{24}\text{Mg}$ ,  $^{28}\text{Si} + ^{28}\text{Si}$ ) and at different incident energies (1.5 to 2.2. times Coulomb barrier) [26–36]. At these incident energies, the incident flux get trapped that results in the formation of compound nucleus, which is in addition to a significant large angle scattering cross-sections. For light masses ( $A < 44$ ), the compound nucleus decays by the emission of light particles and  $\gamma$ -rays. An experimental measure of this so called particle evaporation residue is the compound nucleus fusion cross-section. For heavier systems, such as  $^{56}\text{Ni}$ , a significant decay strength to heavier fragments is also observed which could apparently not arise from a direct reaction mechanism because of large mass asymmetry differences between the entrance and exit channels. The measured angular distributions and energy spectra are consistent with fission like decays of the respective compound systems.

The measured mass distribution for  $^{56}\text{Ni}$  shows a preferential decays to channels comprising  $\alpha$ -nuclei  $^{16}\text{O}$ ,  $^{20}\text{Ne}$ ,  $^{24}\text{Mg}$  and  $^{28}\text{Si}$ , and their complimentary fragments [34–36], independent of the entrance channel nuclei and centre-of-mass energy  $E_{cm}$ . Such an  $\alpha$ -structure is associated with the shell effects in the potential energy surface of the compound nucleus [35], though these are almost zero at the compound nucleus excitation energies involved. Such an  $\alpha$ -nucleus structure in the measured mass distribution of  $^{56}\text{Ni}$  has its origin in the macroscopic energy [38].

Cluster decay is studied for  $^{56}\text{Ni}$ , when formed as an excited compound system in heavy-ion collisions. Since  $^{56}\text{Ni}$  has negative  $Q_{out}$ , and hence stable against both fission and cluster decay processes. However, if it is produced in heavy-ion reactions depending on the incident energy and angular momentum, the excited compound system could either fission, decay via cluster emissions or results in resonance phenomenon. The negative  $Q_{out}$  is different for various exit channels and hence would decay only if it were produced with sufficient compound nucleus excitation energy  $E_{CN}^*$  ( $= E_{cm} + Q_{in}$ ), to compensate for negative  $Q_{out}$ , the deformation energy of the fragments  $E_d$ , their total kinetic energy ( $TKE$ ) and the total excitation energy ( $TXE$ ), in the exit channel as:

$$E_{CN}^* = |Q_{out}| + E_d + TKE + TXE. \quad (7)$$

(see Fig. 1, where  $E_d$  is neglected because the fragments are considered to be spherical). Here  $Q_{in}$  adds to the entrance channel kinetic energy  $E_{cm}$  of the incoming nuclei in their ground states.

Section II gives some details of the Skyrme energy density model and preformed cluster model and its simplification to unified fission model. Our calculations for the decay half-life times of  $^{56}\text{Ni}^*$  compound system and a discussion of the results are presented in Section III. Finally, the results are summarized in Section IV.

## II. MODEL

### A. Skyrme Energy Density Model

In the Skyrme Energy Density Model (SEDM), the real part of interaction potential  $V_N(R)$  is defined as difference between energy expectation value  $E$  of the whole system calculated at a finite distance  $R$  and at infinity [17, 21].

$$V_N(r) = E(r) - E(\infty), \quad (8)$$

with

$$E = \int H(\vec{r}) d\vec{r}. \quad (9)$$

In this formalism, the energy density functional  $H(\vec{r})$  read as;

$$\begin{aligned} H(\rho, \tau, \vec{J}) = & \frac{\hbar^2}{2m}\tau + \frac{1}{2}t_0[(1 + \frac{1}{2}x_0)\rho^2 - (x_0 + \frac{1}{2})(\rho_n^2 + \rho_p^2)] + \frac{1}{4}(t_1 + t_2)\rho\tau \\ & + \frac{1}{8}(t_2 - t_1)(\rho_n\tau_n + \rho_p\tau_p) + \frac{1}{16}(t_2 - 3t_1)\rho\nabla^2\rho \\ & + \frac{1}{32}(3t_1 + t_2)(\rho_n\nabla^2\rho_n + \rho_p\nabla^2\rho_p) + \frac{1}{4}t_3\rho_n\rho_p\rho \\ & - \frac{1}{2}W_0(\rho\vec{\nabla}\cdot\vec{J} + \rho_n\vec{\nabla}\cdot\vec{J}_n + \rho_p\vec{\nabla}\cdot\vec{J}_p). \end{aligned} \quad (10)$$

Here  $\rho = \rho_n + \rho_p$  is the nucleon density taken to be two-parameter Fermi density and  $\vec{J} = \vec{J}_n + \vec{J}_p$  is the spin density which was generalized by Puri et al. [17], for spin-unsaturated nuclei. The remaining term is the kinetic energy density  $\tau = \tau_n + \tau_p$ . The Coulomb effects are neglected in the above energy density functional, but will be added explicitly. In Eq. (10), six parameters  $t_0$ ,  $t_1$ ,  $t_2$ ,  $t_3$ ,  $x_0$ , and  $W_0$  are fitted by different authors to obtain the best description of the various ground state properties for a large number of nuclei. As discussed in the introduction, these different parameterizations have been labeled as S, SI, SII, SIII etc..

The evaluation of kinetic energy density term was done within the Thomas-Fermi (TF) approximation which is a well known alternative to the Hartree-Fock method. As shown by various authors [41], the kinetic energy density  $\tau$  can be separated into volume term  $\tau_0$  and surface term plus reminder. In other words,

$$\tau = \tau_0 + \tau_\lambda + \dots \quad (11)$$

In the first order approximation, one can limit to  $\tau_0$  term only. The volume term  $\tau_0$  in this approximation is given by

$$\tau_0 = \frac{3}{5} \left( \frac{3}{2}\pi^2 \right)^{\frac{2}{3}} \rho^{\frac{5}{3}}. \quad (12)$$

The kinetic energy density  $\tau$  [41, 42], after including additional surface effects is

$$\tau = \tau_0 + \lambda \frac{(\vec{\nabla}\rho)^2}{\rho}, \quad (13)$$

here,  $\lambda$  is a constant whose value has been a point of controversy and different authors have suggested different values, lying between 1/36 and 9/36. The above Thomas-Fermi approximation for  $\tau$  reduces the dependence of energy density  $H(\vec{r})$  to nucleon density  $\rho$  only. The exchange effects due to anti-symmetrization can be assimilated to reasonable extent when Eq. (13) is used [17]. We apply the standard Fermi mass density distribution for nucleonic density:

$$\rho_i(R) = \frac{\rho_{0i}}{1 + \exp\left\{\frac{R-R_{0i}}{a_i}\right\}}, \quad -\infty \leq R \leq \infty \quad (14)$$

The average central density  $\rho_{0i}$  given by [16]

$$\rho_{0i} = \frac{3A_i}{4\pi R_{0i}^3} \frac{1}{\left[1 + \frac{\pi^2 a_i^2}{R_{0i}^2}\right]}, \quad (15)$$

$R_{0i}$  and  $a_i$  are, respectively, the half-density radii and surface diffuseness parameters taken from Refs.[17, 43]. For the details of the model, reader is referred to Ref. [17].

## B. The Preformed Cluster Model

For the cluster decay studies, we use the Preformed Cluster Model (PCM) [8–10]. This model, based on the quantum mechanical fragmentation theory [44–47], uses the decoupled approximation to  $\eta$ - and  $R$ -motions. The decay constant ( $\Lambda$ ) in the PCM is defined as,

$$\Lambda = \nu_0 P P_0, \quad \left( \text{or } T_{1/2} = \frac{\ln 2}{\Lambda} \right), \quad (16)$$

here  $\nu_0$  is the assault frequency with which the cluster hits the barrier,  $P$  is the probability of penetrating the barrier and  $P_0$  is the preformation probability. Thus, in contrast to the unified fission models [5–7], the two fragments in PCM are considered to be formed at a relative separation co-ordinate  $R$  before the penetration of the potential barrier with probability  $P_0$ . The Schrödinger equation in terms of  $\eta$  and  $R$  coordinates as:

$$H(\eta, R)\psi(\eta, R) = E\psi(\eta, R), \quad (17)$$

The above equation can be solved in a decoupled approximation [8, 9], for which the Hamiltonian takes the form:

$$H = -\frac{\hbar^2}{2\sqrt{B_{\eta\eta}}} \frac{\partial}{\partial\eta} \frac{1}{\sqrt{B_{\eta\eta}}} \frac{\partial}{\partial\eta} - \frac{\hbar^2}{2\sqrt{B_{RR}}} \frac{\partial}{\partial R} \frac{1}{\sqrt{B_{RR}}} \frac{\partial}{\partial R} + V(\eta) + V(R). \quad (18)$$

Since the potentials are calculated within the Strutinsky re-normalization procedure ( $V = V_{Macro} + \delta U$ ) by using an appropriate liquid drop model potential  $V_{Macro}$  and asymmetric two center shell model for shell corrections  $\delta U$ , are nearly independent of the relative separation coordinate  $R$ ,  $R$  can be taken as a time independent parameter. For the Hamiltonian Eq. (18), the Schrödinger Eq. (17) can be separated in two co-ordinates  $\eta$  and  $R$  as follows:

$$\left[ -\frac{\hbar^2}{2\sqrt{B_{\eta\eta}}} \frac{\partial}{\partial\eta} \frac{1}{\sqrt{B_{\eta\eta}}} \frac{\partial}{\partial\eta} + V(\eta) \right] \psi(\eta) = E_\eta \psi(\eta), \quad (19)$$

and

$$\left[ -\frac{\hbar^2}{2\sqrt{B_{RR}}} \frac{\partial}{\partial R} \frac{1}{\sqrt{B_{RR}}} \frac{\partial}{\partial R} + V(R) \right] \psi(R) = E_R \psi(R), \quad (20)$$

with  $\psi(\eta, R) = \psi(\eta) \psi(R)$  and  $E = E_\eta + E_R$ .

The fragmentation potential (or collective potential energy)  $V(\eta)$ , appearing in Eq. (19), is calculated as,

$$V(\eta) = -\sum_{i=1}^2 \left[ V_{Macro}(A_i, Z_i) + \delta U_i \exp\left(-\frac{T^2}{T_0^2}\right) \right] + \frac{Z_1 \cdot Z_2 e^2}{R} + V_N(R) + V_\ell, \quad (21)$$

where the theoretical binding energies ( $V = V_{Macro} + \delta U$ ) are taken from Möller et al. [48]. The charges  $Z_i$  in Eq. (21) are fixed by minimizing the potential  $V(\eta_Z)$ , defined by Eq. (21) without  $V_N(R)$  in  $\eta_Z$  co-ordinates. The shell corrections  $\delta U$  are considered to vanish exponentially for  $E_{CN}^* \geq 60$  MeV, giving  $T = 1.5$  MeV. At higher excitation energies, the shell corrections vanish completely and only the liquid drop part of energy is present. The additional attraction due to nuclear interaction potential  $V_N(R)$  is calculated within SEDM potential. The rotational energy due to angular momentum effects  $V_\ell (= \hbar^2 \ell(\ell+1)/2\mu R^2)$  is not added here since its contribution to the structure yields is shown to be small for lighter systems [46]. The nuclear temperature  $T$  (in MeV), is related approximately to the excitation energy  $E_{CN}^*$ , as:

$$E_{CN}^* = \frac{1}{9} A T^2 - T \quad (\text{in MeV}). \quad (22)$$

The kinetic energy part of the Hamiltonian in Eq. (19) comes through the mass parameter  $B_{\eta\eta}$  which is calculated using the classical mass parameter of Kröger and Scheid [49], based on the hydrodynamical flow. The mass parameter  $B_{\eta\eta}$  reads as:

$$B_{\eta\eta} = \frac{AmR_{min}^2}{4} \left[ \frac{v_t(1+\beta)}{v_c(1+\delta^2) - 1} \right], \quad (23)$$

with

$$\beta = \frac{R_c}{2R_{min}} \left[ \frac{1}{1 + \cos \theta_1} \left( 1 - \frac{R_c}{R_1} \right) + \frac{1}{1 + \cos \theta_2} \left( 1 - \frac{R_c}{R_2} \right) \right], \quad (24)$$

$$\delta = \frac{1}{2R_{min}} [(1 - \cos \theta_1)(R_1 - R_c) + (1 - \cos \theta_2)(R_2 - R_c)], \quad (25)$$

$$v_c = \pi R_c^2 R_{min}, \quad R_c = 0.4R_2, \quad (26)$$

and  $v_t = v_1 + v_2$ , is the total conserved volume.

Solving Eq. (19) numerically,  $|\psi(\eta)|^2$  gives the probability of finding the mass fragmentation  $\eta$  at a fixed position  $R$ , on the decay path. Normalizing and scaling  $|\psi(\eta)|^2$  to give the fractional mass yield for each fragment in the ground state decay as:

$$P_0(A_i) = |\psi(\eta)|^2 \sqrt{B_{\eta\eta}(\eta)} \left( \frac{4}{A_i} \right), \quad (i = 1 \text{ or } 2). \quad (27)$$

The nuclear temperature effects in Eq. (27) are also included through a Boltzmann-like function,

$$|\psi(\eta)|^2 = \sum_{\nu=0}^{\infty} |\psi(\eta)|^2 \exp\left(-\frac{E_\eta}{T}\right). \quad (28)$$

For  $R$ -motion, instead of solving the stationary Schrödinger Eq. (20), the WKB action integral was solved for the penetration probability  $P$  [50]. For each  $\eta$ -value, the potential  $V(R)$  is calculated by using SEDM for  $R \geq R_d$ , with  $R_d = R_{min} + \Delta R$  and for  $R \leq R_d$ , it is parameterized simply as a polynomial of degree two in  $R$ :

$$V(R) = \begin{cases} |Q_{out}| + a_1(R - R_0) + a_2(R - R_0)^2 & \text{for } R_0 \leq R \leq R_d, \\ V_N(R) + Z_1 \cdot Z_2 e^2 / R & \text{for } R \geq R_d, \end{cases} \quad (29)$$

where  $R_0$  is the parent nucleus radius and  $\Delta R$  is chosen for smooth matching between the real potential and the parameterized potential (with second-order polynomial in  $R$ ). A typical scattering potential, calculated by using Eq. (29) is shown in Fig. 1, with tunneling paths and the characteristic quantities also marked. Here we choose the first (inner) turning point  $R_a$  at the minimum configuration i.e.  $R_a = R_{min}$  (corresponding to  $V_{min}$ ) with potential at this  $R_a$ -value as  $V(R_a = R_{min}) = \bar{V}_{min}$  (displayed in Fig. 1) and the outer turning point  $R_b$  to give the  $Q_{eff}$ -value of the reaction ( $Q_{eff} = |Q_{out}| + TKE$ ) i.e.  $V(R_b) = Q_{eff}$ . This means that the transmission probability  $P$  with the de-excitation probability,  $W_i = \exp(-bE_i)$  taken as unity, can be written as:

$$P = P_i P_b, \quad (30)$$

where  $P_i$  and  $P_b$  are calculated by using WKB approximation, as:

$$P_i = \exp \left[ -\frac{2}{\hbar} \int_{R_a}^{R_i} \{2\mu[V(R) - V(R_i)]\}^{1/2} dR \right], \quad (31)$$

and

$$P_b = \exp \left[ -\frac{2}{\hbar} \int_{R_i}^{R_b} \{2\mu[V(R) - Q_{eff}]\}^{1/2} dR \right], \quad (32)$$

here  $R_a$  and  $R_b$  are, respectively, the first and second turning points. This means that the tunneling begins at  $R = R_a$  ( $= R_{min}$ ) and terminates at  $R = R_b$ , with  $V(R_b) = Q_{eff}$ . The integrals of Eqs. (31) and (32) are solved analytically by parameterizing the above calculated potential  $V(R)$ .

The assault frequency or the barrier impinging frequency  $\nu_0$  in Eq. (16), is given simply as,

$$\nu_0 = \frac{v}{R_0} = \frac{(2E_2/\mu)^{1/2}}{R_0}, \quad (33)$$

where  $E_2 = \frac{A_1}{A}Q_{eff}$  is the kinetic energy of the emitted cluster, with  $Q_{eff}$  shared between the two fragments and  $\mu = m(\frac{A_1A_2}{A})$  is the reduced mass.

The PCM can be simplified to unified fission model (UFM), if preformation probability  $P_0 = 1$  and the penetration path is straight to  $Q_{eff}$ -value.

### III. RESULTS AND DISCUSSIONS

The calculations are made in two steps: In the first steps, we studied the role of different Skyrme forces in the cluster decay of  $^{56}\text{Ni}^*$  and in the second step, effect of surface correction term  $\lambda$  is analyzed.

Fig. 1 shows the characteristic scattering potential for the cluster decay of  $^{56}\text{Ni}^*$  into  $^{16}\text{O} + ^{40}\text{Ca}$  channel as an illustrative example. In the exit channel for the compound nucleus to decay, the compound nucleus excitation energy  $E_{CN}^*$  goes in compensating the negative  $Q_{out}$ , the total excitation energy  $TXE$  and total kinetic energy  $TKE$  of the two outgoing fragments as the effective  $Q$ -value (i.e.  $TKE = Q_{eff}$  in the cluster decay process). In addition, we plot the penetration paths for PCM and UFM. For PCM, we begin the penetration path at  $R_a = R_{min}$  with potential at this  $R_a$ -value as  $V(R_a = R_{min}) = \bar{V}_{min}$  and ends at  $R = R_b$ , corresponding to  $V(R = R_b) = Q_{eff}$ , whereas for UFM, we begin at  $R_a$  and end at  $R_b$  both corresponding to  $V(R_a) = V(R_b) = Q_{eff}$ . We have chosen only the case of different  $Q_{eff}$  (listed in Table 1), for different cluster decay products to satisfy the arbitrarily chosen relation  $Q_{eff} = 0.4(28 - |Q_{out}|)$  MeV, as it is more realistic [38].

#### A. Role of Different Skyrme Forces

Figs. 2(a) and (b) shows the fragmentation potential  $V(\eta)$  and fractional yield at  $R = R_{min}$  with  $V(R_{min}) = \bar{V}_{min}$ . The classical hydrodynamical mass parameter  $B_{\eta\eta}$  of Kröger and Scheid [49] used in the calculation of preformation probability. The fractional yields are calculated within PCM at  $T = 3.0$  MeV using different Skyrme forces for  $^{56}\text{Ni}^*$ . From the figure, we observe that different Skyrme forces do not alter the transfer structure of fractional yields. The Skyrme force parameters have marginal role to play. Some variations in the absolute values are however visible [51]. The fine structure is not at all disturbed for different sets of Skyrme forces.

The results for the cluster decay half-lives in  $^{56}\text{Ni}^*$  are quantified by the following quantity as:

$$[\log T_{1/2}] \% = \frac{(\log T_{1/2})^i - (\log T_{1/2})^{SIII}}{(\log T_{1/2})^{SIII}} \times 100, \quad (34)$$

where  $i$  stands for different sets of Skyrme force parameters and SIII for one set of Skyrme force parameters, which is widely used. Here, the strength parameter of surface correction is taken as zero (i.e.  $\lambda = 0$ ).

In Fig. 3(a) and (b), we display the quantified results using Eq. (34) for  $\log T_{1/2}$  within PCM and UFM models as a function of cluster mass  $A_2$ . The role of temperature  $T$  (or excitation energy  $E_{CN}^*$ ) enters only in the PCM via preformation probability  $P_0$ . These variation in the cluster decay half-lives for different clusters lies within  $\pm 10\%$  for PCM and  $\pm 15\%$  for UFM. This amount is significant once we understand cluster decay probabilities can be measured with great accuracy in the literature.

#### B. Role of Strength Parameter of Surface Correction ( $\lambda$ )

The effect of different  $\lambda$ -values for the heavy-ion nuclear potential is analyzed in Refs. [17, 52], suggesting that different  $\lambda$ -value, can alter the depth of the nuclear potential  $V_N$  significantly. In Ref. [17], it was shown that the barrier heights gets lowered whereas the fusion barrier position shifts outward where stronger role of  $\lambda$  is taken into account. The effect of this strength parameter  $\lambda$  for additional surface effects in the decay calculations has yet not been studied in the literature. In this subsection, we plan to study the effect of strength parameter of surface correction

on cluster decay half-lives by taking different  $\lambda$ -values (equal to 0, 1/36, 2/36, 3/36, 4/36, and 5/36) in SEDM for the compound system  $^{56}\text{Ni}^*$ .

In Fig. 4, the scattering potential for different values of surface correction factor  $\lambda$  is plotted as a function of internuclear distance  $R$ . One observes from the figure that variation in the  $\lambda$ -value changes the interior part of the scattering potential thereby changing the penetration probability.

In Fig 5(a) and (b), we show the fragmentation potential  $V(\eta)$  and fractional mass distribution yield at  $R = R_{min}$  with  $V(R_{min}) = \bar{V}_{min}$ . The fractional yields are calculated within PCM at  $T = 3.0$  MeV using different values of surface correction factor for  $^{56}\text{Ni}^*$ . From figure, we observe that different values of  $\lambda$  changes the fractional yield to large extent but do not alter its transfer structure. The fine structure is not at all disturbed for different values of surface correction factor.

The results for the cluster decay half-lives in  $^{56}\text{Ni}^*$  are quantified by the following quantity as:

$$[\log T_{1/2}] \% = \frac{(\log T_{1/2})^i - (\log T_{1/2})^{\lambda=0}}{(\log T_{1/2})^{\lambda=0}} \times 100, \quad (35)$$

where  $i$  stands for different  $\lambda$ -values of the strength parameter of surface correction. Skyrme force SIII is employed for these calculations. In Fig. 6, we display the quantified results using Eq. (35) for the percentage variation of  $\log T_{1/2}$  within PCM and UFM as a function of cluster mass  $A_2$ . The variation in the cluster decay half-lives for different clusters lies within  $\pm 10\%$  for both PCM and UFM. Together with the effect of different Skyrme forces, one can see that the net effect of different Skyrme forces as well as surface corrections has sizable effect on the cluster decay half-life times.

#### IV. SUMMARY

We here reported the role of different Skyrme forces as well as surface corrections in the cluster decay constant calculations. Our studies revealed that the effect of different Skyrme forces on the cluster decay half-life times is about  $\pm 15\%$ , whereas it is  $\pm 10\%$  in the case of surface corrections.

This work was supported by a research grant from the Department of Atomic Energy, Government of India.

- 
- [1] J.M.B. Shorto *et al.*, *Phys. Rev.* **C81**, 044601 (2010); I. Dutt, R.K. Puri *ibid.* **81**, 047601 (2010); *ibid.* **81**, 044615 (2010); *ibid.* **81**, 064609 (2010); *ibid.* **81**, 064608 (2010).
  - [2] C. Xu, B.A. Li *Phys. Rev.* **C 81**, 044603 (2010); S. Kumar *ibid.* **78**, 064602 (2008); *ibid.* **81**, 014611 (2010); *ibid.* **81**, 014601 (2010); Y.K. Vermani *et al.*, *J. Phys. G: Nucl. Part. Phys.* **36**, 105103 (2010); *ibid.* **37**, 015105 (2010); *ibid.* *Europhys. Lett.* **85**, 62001 (2009); *ibid.* *Phys. Rev.* **C 79**, 064613 (2009); A. Sood *et al.*, *ibid.* **79**, 064618 (2009); S. Gautam *et al.*, *J. Phys. G: Nucl. Part. Phys.* **37**, 085102 (2010); Y. Vermani, R.K. Puri *Nucl. Phys.* **A**, (2010) in press.
  - [3] S.K. Patra *et al.*, *Phys. Rev.* **C 80**, 034612 (2009); S.K. Arun *et al.*, *ibid.* **80**, 034317 (2009); *ibid.* **79**, 064616 (2009); R. Kumar *et al.*, *ibid.* **79**, 034602 (2009).
  - [4] K.P. Santhosh *et al.*, *J. Phys. G: Nucl. Part. Phys.* **36**, 115101 (2009); *ibid.* **36**, 015107 (2009); *Pramana J. Phys.* **59**, 599 (2002).
  - [5] D.N. Poenaru, W. Greiner, R. Gherghescu, *Phys. Rev.* **C47**, 2030 (1993); H.F. Zhang *et al.*, *ibid.* **80**, 037307 (2009).
  - [6] R.K. Gupta *et al.*, *J. Phys. G: Nucl. Part. Phys.* **26**, L23 (2000); B. Buck, A.C. Merchant, S.M. Perez, *Nucl. Phys.* **A512**, 483 (1990); B. Buck, A.C. Merchant, *J. Phys. G: Nucl. Part. Phys.* **16**, L85 (1990).
  - [7] A. Sandulescu *et al.*, *Int. J. Mod. Phys.* **E1**, 379 (1992); R.K. Gupta, *et al.*, *J. Phys. G: Nucl. Part. Phys.* **19**, 2063 (1993); *Phys. Rev.* **C56**, 3242 (1997).
  - [8] R.K. Gupta, *5th International Conference on Nuclear Reaction Mechanisms, Varenna, Italy*, p. 416 (1988).
  - [9] S.S. Malik, R. K. Gupta, *Phys. Rev.* **C39**, 1992 (1989); *ibid.* **C50**, 2973 (1994); S.S. Malik *et al.*, *Pramana J. Phys.* **32**, 419 (1989); R.K. Puri *et al.*, *Europhys. Lett.* **9**, 767 (1989); R. K. Puri *et al.*, *J. Phys. G: Nucl. Part. Phys.* **18**, 903 (1992).
  - [10] S. Kumar, R.K. Gupta, *Phys. Rev.* **C55**, 218 (1997).
  - [11] W.D. Myers, W.J. Świątecki, *Phys. Rev.* **C62**, 044610 (2000).
  - [12] P.R. Christensen, A. Winther, *Phys. Lett.* **B65**, 19 (1976).
  - [13] J. Blocki *et al.*, *Ann. Phys.* **105**, 427 (1977).
  - [14] R. Bass, *Nucl. Phys.* **A231**, 45 (1974); *Phys. Rev. Lett.* **39**, 265 (1977).
  - [15] V.Y. Denisov, *Phys. Lett.* **B526**, 315 (2002); V.Y. Denisov, S. Hofmann, *Phys. Rev.* **C61**, 034606 (2000); *ibid.* **76**, 014602 (2007); *ibid.* **81**, 034613 (2010); *ibid.* **81**, 025805 (2010).
  - [16] D.M. Brink, F. Stancu, *Nucl. Phys.* **A243**, 175 (1975); F. Stancu, D.M. Brink, *ibid.* **A270**, 236 (1976).

- [17] R.K. Puri *et al.*, *Eur. Phys. J.* **A23**, 429 (2005); R. Arora *et al.*, *ibid.* **8**, 103 (2000); R.K. Puri *et al.*, *ibid.* **3**, 277 (1998); R.K. Puri *et al.*, *Phys. Rev.* **C51**, 1568 (1995); *ibid.* **45**, 1837 (1992); *ibid.* **43**, 315 (1991); *ibid. J. Phys. G: Nucl. Part. Phys.* **18**, 903 (1992); R.K. Puri, R.K. Gupta, *Int. J. Mod. Phys.* **E1**, 269 (1992).
- [18] A. Dobrowolski, K. Pomorski, J. Bartel, *Nucl. Phys.* **A723**, 93 (2003); J. Bartel *et al.*, *Eur. Phys. J.* **A14**, 179 (2002); M. Liu *et al.*, *Nucl. Phys.* **A768**, 80 (2006); N. Wang, J.Q. Li, E.G. Zhao, *Phys. Rev.* **C74**, 044604 (2006).
- [19] M. Brack, C. Guet, H.-B. Håkansson, *Phys. Rep.* **123**, 275 (1985).
- [20] T.H.R. Skyrme, *Phil. Mag.* **1**, 1043 (1956); *Nucl. Phys.* **9**, 615 (1959).
- [21] D. Vautherin, D.M. Brink, *Phys. Rev.* **C5**, 626 (1972).
- [22] Q. Shen, Y. Han, H. Guo, *Phys. Rev.* **C80**, 024604 (2009); Z. Feng, G. Jin, F. Zhang, *Nucl. Phys.* **A802**, 91 (2008).
- [23] S. Kumar *et al.*, *Phys. Rev.* **C58**, 3494 (1998); *ibid.* **C58**, 1618 (1998); J. Singh *et al.*, *Phys. Rev.* **C62**, 044617 (2000); J. Dhawan *et al.*, *Phys. Rev.* **C75**, 057601 (2007); R.K. Puri *et al.*, *Nucl. Phys.* **A575**, 733 (1994); D.T. Khoa *et al.*, *Nucl. Phys.* **A542**, 671 (1992); S.W. Huang *et al.*, *Phys. Lett.* **B298**, 41 (1993); G. Batko *et al.*, *J. Phys. G: Nucl. Part. Phys.* **20**, 461 (1994); S.W. Huang *et al.*, *Prog. Part. Nucl. Phys.* **30**, 105 (1993); E. Lehmann *et al.*, *Prog. Part. Nucl. Phys.* **30**, 219 (1993).
- [24] R.K. Puri *et al.*, *Phys. Rev.* **C54**, R28 (1996); *ibid. J. Comput. Phys.* **162**, 245 (2000); A. Sood *et al.*, *Phys. Rev.* **C70**, 034611 (2004); *ibid. Phys. Lett.* **B594**, 260 (2004); P.B. Gossiaux *Nucl. Phys.* **A619**, 379 (1997); C. Fuchs *et al.*, *J. Phys. G: Nucl. Part. Phys.* **22**, 131 (1996); E. Lehmann *et al.*, *Z. Phys* **A355** 55 (1996); E. Lehmann *et al.*, *Phys. Rev.* **C51**, 2113 (1995); S. Kumar *et al.*, *Phys. Rev.* **C58**, 320 (1998); *Phys. Rev.* **C57**, 2744 (1998).
- [25] G. Lingxiao, Z. Yizhong, W. Nörenberg, *Nucl. Phys.* **A459**, 77 (1986); Li G. Qiang, *J. Phys. G: Nucl. Part. Phys.* **17**, 1 (1991).
- [26] S.J. Sanders, A. S. de Toledo, C. Beck, *Phys. Rep.* **311**, 487 (1999).
- [27] S.J. Sanders *et al.*, *Phys. Rev. Lett.* **59**, 2856 (1987); *ibid.* **61**, 2154 (1988).
- [28] S.J. Sanders, *Phys. Rev.* **C44**, 2676 (1991).
- [29] R. Nouicer *et al.*, *Phys. Rev.* **C60**, 041303 (1999).
- [30] C. Beck *et al.*, *Phys. Rev.* **C63**, 014607 (2001).
- [31] S. Thummerer *et al.*, *J. Phys. G: Nucl. Part. Phys.* **27**, 1405 (2001).
- [32] C. Bhattacharya *et al.*, *Phys. Rev.* **C57**, 203 (2001); *ibid.* **C65**, 014611 (2002).
- [33] S.J. Sanders *et al.*, *Phys. Rev.* **C34**, 1746 (1986).
- [34] R.R. Betts, *Conference on Resonances in Heavy Ion Reactions, Bad Hönnef: Lecture Notes in Physics*, Vol. **156**, edited by K. A. Eberhardt, Springer, Berlin, p. 185 (1981).
- [35] S.J. Sanders *et al.*, *Phys. Rev.* **C40**, 2091 (1989).
- [36] S.J. Sanders *et al.*, *Phys. Rev.* **C49**, 1016 (1994).
- [37] R.K. Gupta *et al.*, *Phys. Rev.* **C68**, 014610 (2003).
- [38] M.K. Sharma, R.K. Gupta, W. Scheid, *J. Phys. G: Nucl. Part. Phys.* **26**, L45 (2000).
- [39] T. Matsuse *et al.*, *Phys. Rev.* **C55**, 1380 (1997).
- [40] B. Shivakumar *et al.*, *Phys. Rev.* **C35**, 1730 (1987).
- [41] P. Chattopadhyay, R.K. Gupta, *Phys. Rev.* **C30**, 1191 (1984), and earlier references therein.
- [42] C.F. von Weizsäcker, *Z. Phys.* **96**, 431 (1935).
- [43] L.R.B. Elton, *Nuclear sizes*, Oxford University Press, London (1961); H.de Vries, C.W. de Jager, C.de Vries, *At. Data Nucl. Data Tables* **36**, 495 (1987).
- [44] R.K. Gupta *et al.*, *J. Phys. G: Nucl. Part. Phys.* **26**, L23 (2000).
- [45] R.K. Gupta, W. Scheid, W. Greiner, *Phys. Rev. Lett.* **35**, 353 (1975).
- [46] D.R. Saroha, N. Malhotra, R.K. Gupta, *J. Phys. G: Nucl. Part. Phys.* **11**, L27 (1985).
- [47] J. Maruhn, W. Greiner, *Phys. Rev. Lett.* **32**, 548 (1974).
- [48] P. Möller *et al.*, *At. Data Nucl. Data Tables* **59**, 185 (1995).
- [49] H. Kröger, W. Scheid, *J. Phys. G: Nucl. Part. Phys.* **6**, L85 (1980).
- [50] R.K. Gupta, W. Greiner, *Int. J. Mod. Phys.* **E3**, 335 (1994).
- [51] N.K. Dhiman, R.K. Puri, *1st Chandigarh Science Congress*, Vol. **IA**, p. 226, March 10-11 (2007).
- [52] N.K. Dhiman, R.K. Puri, *Acta Phys. Pol.* **B37**, 1855 (2006).

TABLE I: The calculated characteristic quantities for cluster decay of  $^{56}\text{Ni}^*$  compound system for fragment masses  $A_2 \geq 16$ , with excitation energies  $E^* = Q_{eff} + |Q_{out}|$ .

Cluster + Daughter	$ Q_{out} $ (MeV)	$Q_{eff}$ (MeV)	$E^*$ (MeV)
$^{16}\text{O} + ^{40}\text{Ca}$	-14.12	5.55	19.67
$^{18}\text{Ne} + ^{38}\text{Ar}$	-22.23	2.31	24.54
$^{20}\text{Ne} + ^{36}\text{Ar}$	-17.12	4.35	21.47
$^{22}\text{Mg} + ^{34}\text{S}$	-24.58	1.37	25.95
$^{24}\text{Mg} + ^{32}\text{S}$	-16.57	4.57	21.14
$^{26}\text{Si} + ^{30}\text{Si}$	-23.57	1.77	25.34
$^{28}\text{Si} + ^{28}\text{Si}$	-12.20	6.32	18.52

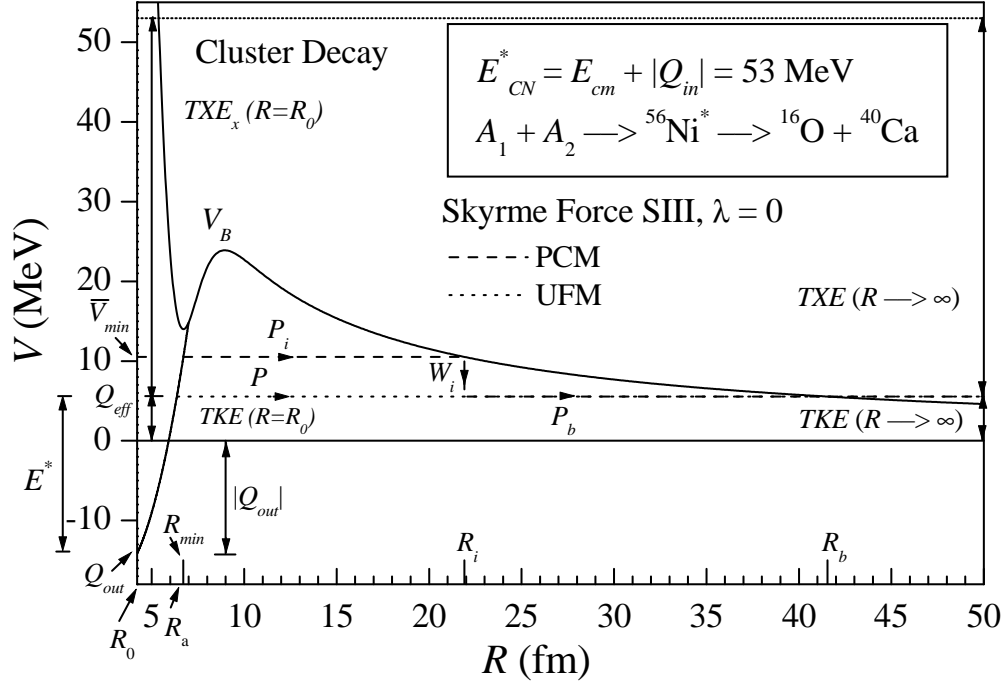


FIG. 1: The scattering potential  $V(R)$  (in MeV) for cluster decay of  ${}^{56}\text{Ni}^*$  into  ${}^{16}\text{O} + {}^{40}\text{Ca}$  channel using Skyrme force SIII, with  $\lambda = 0$ . The distribution of compound nucleus excitation energy  $E_{CN}^*$  at both the initial ( $R = R_0$ ) and asymptotic ( $R \rightarrow \infty$ ) stages and  $Q$ -values are shown. The decay path for both PCM and UFM models is also displayed.

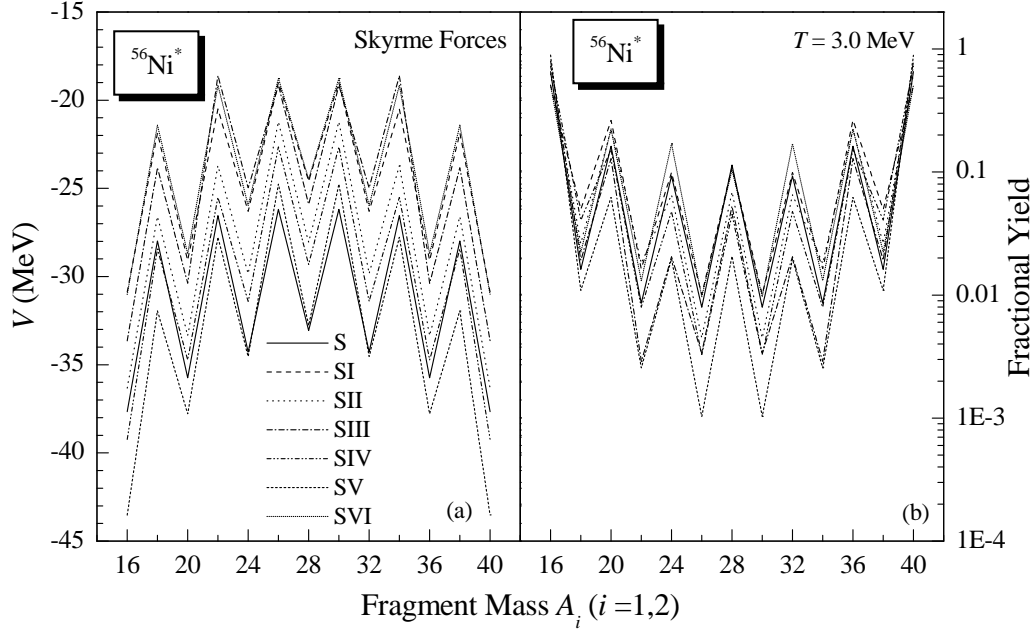


FIG. 2: (a) The fragmentation potential  $V(\eta)$  and (b) calculated fission mass distribution yield with different Skyrme forces at  $T = 3.0$  MeV.

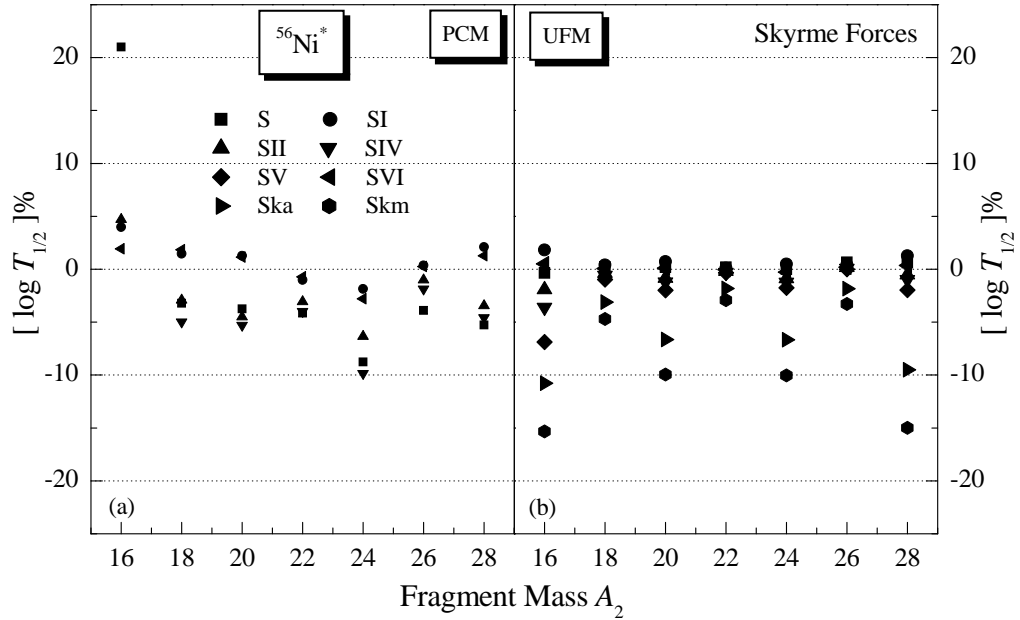


FIG. 3: Percentage variation of  $\log T_{1/2}$  for different Skyrme forces w.r.t. SIII force.

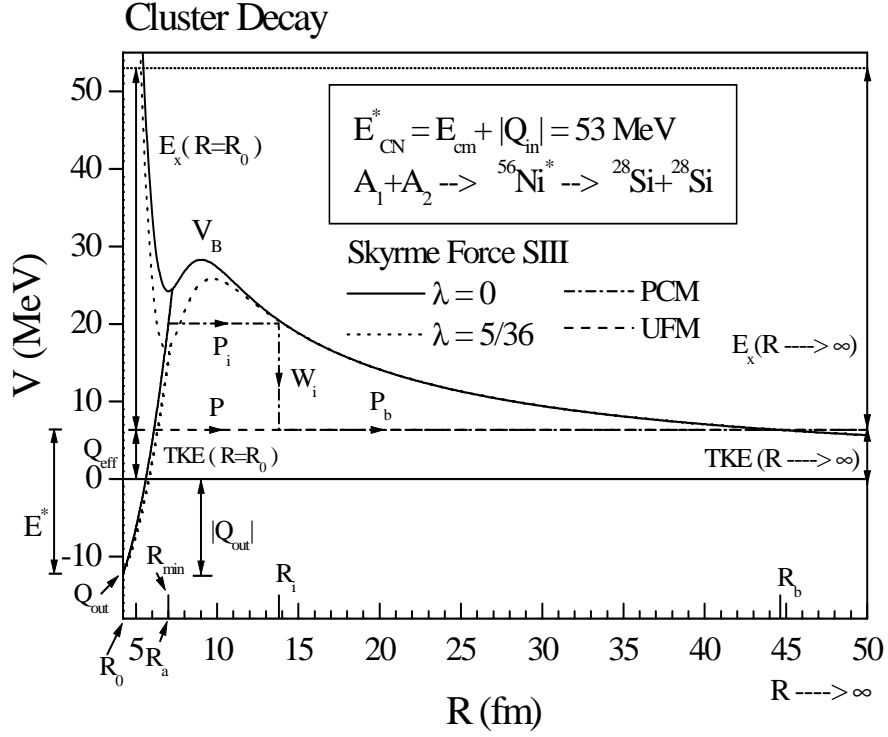


FIG. 4: Same as Fig 1, but for different values of surface correction factor ( $\lambda$ ).

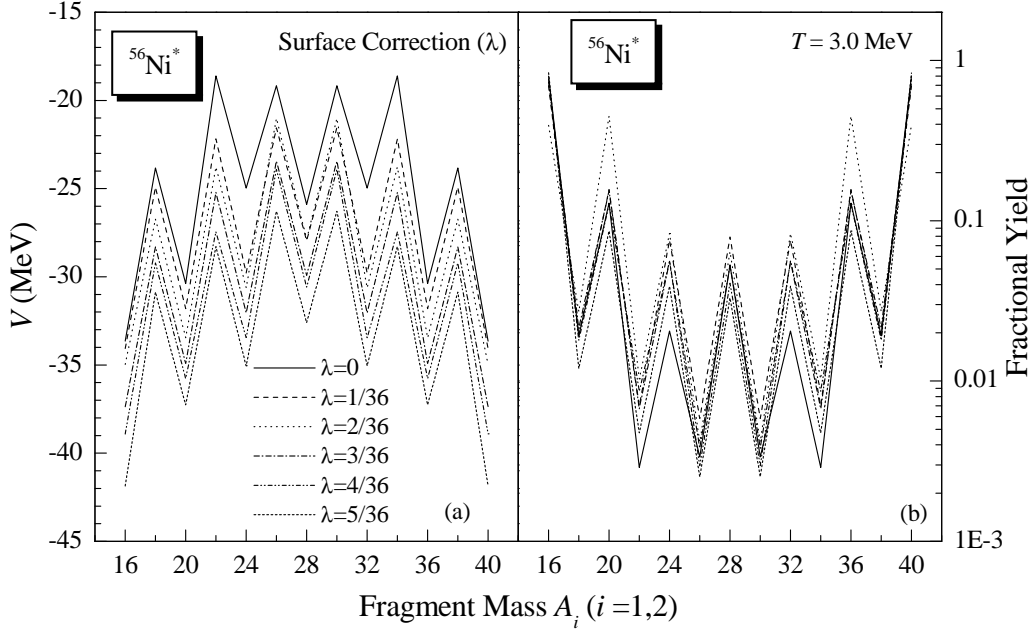


FIG. 5: Same as Fig 2, but for different values of surface correction factor ( $\lambda$ ).

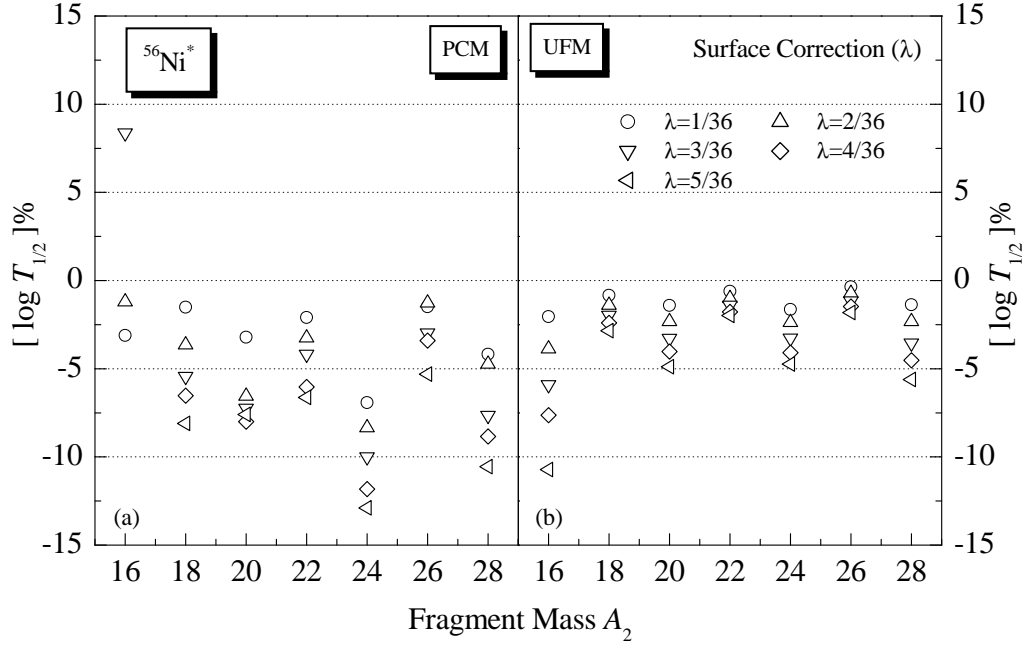


FIG. 6: Same as Fig 3, but for different values of strength parameter of surface correction ( $\lambda \neq 0$ ) w.r.t. surface correction ( $\lambda = 0$ ).